The role of new PET tracers for lung cancer

[1,2] Sachin V Kamat

[1,2] Teresa A Szyszko

[1,2] Manil Subesinghe

[1,2,3] Barbara Malene Fischer

[1,2] Sugama Chicklore

[1,2] Victoria Warbey

[1,2] Gary J.R. Cook

[1]King's College London and Guy's & St Thomas' PET Centre, School of Biomedical Engineering and Imaging Sciences, King's College London, London. SE1 7EH. UK

[2]Department of Cancer Imaging, School of Biomedical Engineering and Imaging Sciences, King's College London, London. UK

[3]Department of Clinical Physiology, Nuclear medicine and PET, Rigshospitalet, Copenhagen University Hospital, Copenhagen, Denmark.

Abstract

^{18}F-Fluorodeoxyglucose (^{18}F-FDG) positron emission tomography–computed tomography (PET/CT) is integral to the investigation and management of suspected or proven lung cancer (1) despite the non-specific nature of the ^{18}F-FDG, which is a glucose analogue. An improved understanding in tumour biology and advances in therapeutic options has driven the need to better characterise tumours, and predict and monitor treatment response to new targeted cancer therapies. Some of the cancer-related cellular processes being investigated include tumour proliferation, amino acid metabolism, tumour hypoxia and angiogenesis. The majority of tracers being used to evaluate these processes remain restricted to preclinical and clinical research. There are also certain receptors which are expressed by specific cancers which can then be targeted by peptides, e.g. neuroendocrine tumours express somatostatin receptors which have an affinity to somatostatin analogues such as DOTA-peptides. ^{68}Ga-DOTA-peptides have an established role in PET imaging, including imaging of carcinoid tumours, but these are not specific to lung lesions.

Introduction

Positron emission tomography-computed tomography (PET/CT) has revolutionised the understanding of disease by enabling the evaluation of disease-specific function at a molecular level. It is established in the characterisation, staging and assessment of response to treatment across a wide range of malignancies, alongside applications in neurological disease, infection and inflammation and cardiac disease. According to the LuCE report on lung cancer (2016) (2), lung cancer is the 4th commonest cancer in the European Union effecting more than 312,000 people every year. ^{18}F-Fluorodeoxyglucose (^{18}F-FDG) PET/CT is used to characterise indeterminate lung nodules, staging of lung cancer and to assess response to variety of treatment options (1).^{18}F-FDG is a glucose analogue that enables assessment of glucose metabolism, with areas of increased uptake, reflecting areas of increased

glycolytic activity. Although, cancers cells have a reliance on glucose to generate energy, manifesting as areas of increased tracer uptake, ^{18}F-FDG uptake can also be seen in areas of infection and inflammation as well as in normal cells. As such, ^{18}F-FDG is sensitive but not specific for the detection of cancer.

A better and improved understanding of cancer biology has led to the development of novel radiopharmaceuticals which might help better characterise tumours and predict response to targeted cancer therapeutics, with the hope of improving the overall diagnostic accuracy of imaging in lung cancer.

Proliferation in lung cancer

Cellular proliferation, leading to an increase in the number of cells as a result of cell growth and multiplication, is one of the hallmarks of malignancy and can be imaged and quantified with ^{18}F-fluorothymidine (^{18}F-FLT). Thymidine kinase-1 (TK-1) is an enzyme which is upregulated during DNA synthesis and cellular growth (3, 4). Uptake of ^{18}F-FLT correlates with the activity of TK-1, as it is phosphorylated to 3-fluorothymidine monophosphate by TK-1 and it is then trapped intracellularly but not incorporated into DNA (5).

11C-thymidine was used initially, however, due to its short half-life of 20 minutes requiring a cyclotron on site for production and rapid metabolism, it is unsuitable for routine use. Thymidine tracers show physiological uptake in bone marrow and liver, which hinders assessment of these organs (6).

In comparison with ^{18}F-FDG, ^{18}F-FLT generally demonstrates a lower degree of tumoural uptake as it is only taken up in the cells that are in the S phase (Fig. 1) (7). Its accumulation in tumour cells directly correlates with histopathological Ki-67 expression in non-small cell lung cancer (NSCLC) (8, 9), thus making it is a more specific oncological tracer than ^{18}F-FDG (Fig. 2).

There is a small body of literature exploring the comparative accuracies of ^{18}F-FLT and ^{18}F-FDG. Buck et al. compared uptake in lung cancer (NSCLC, SCLC and metastases) and showed whilst ^{18}F-FLT uptake was related exclusively to malignant tumours, ^{18}F-FDG uptake was also seen in 4/8 benign lesions (10). The investigators also found that the sensitivity of ^{18}F-FLT for nodal staging was poor (53%), but could be a suitable radiopharmaceutical for investigating brain metastases as there is little background physiological tracer accumulation in the brain (9). They also suggested that ^{18}F-FLT may be the superior tracer for assessment of therapy response and outcome.

In a similar study in 31 patients with NSCLC, Yang et al. reported that the sensitivities of ^{18}F-FLT and ^{18}F-FDG for primary lesions were 74% and 94%, respectively ($p=0.003$) and ^{18}F-FDG was more sensitive in regional nodal staging (11). Tian et al. studied dual tracer imaging of pulmonary nodules with ^{18}F-FLT and ^{18}F-FDG in 55 patients and found the combination to be better than either tracer alone (12). The sensitivity and specificity of ^{18}F-FLT were 68.75% and 76.92% and for ^{18}F-FDG were 87.5% and 58.97%, respectively. The combination of dual-tracer PET/CT improved the sensitivity and specificity up to 100% and 89.74%, respectively.

Other trials evaluated response assessment with FLT alone. Sohn et al. studied gefitinib (an EGFR tyrosine kinase inhibitor) response in patients with advanced adenocarcinoma of the lung measuring changes in ^{18}F-FLT uptake and found that activity on day 7 differed significantly between responders and non-responders (13). Trigonis et al. found, in patients with NSCLC treated with radiotherapy and imaged with ^{18}F-FLT PET, that radiotherapy induced an early significant decrease in tracer uptake, after 5-11 treatment fractions (14).

It has been found that treatment with ADI-PEG20 (arginine deiminase formulated with polyethylene glycol) in ASS 1 (Argininosuccinate synthase) deficient bladder tumours showed a marked reduction in the intracellular levels of thymidine due to the reduction in the TK1 protein levels (15). Utilising 18F-FLT to assess treatment response of NSCLC and mesothelioma with ADI-PEG20 in combination with cisplatin and pemetrexed is encouraging and has shown a significant decrease in tracer uptake at the end of treatment, consistent with human tumour xenograft studies of ADI-PEG20 and the known pharmacology of arginine depletion in ASS1-deficient tumours, suggesting that measuring changes in proliferation with FLT are likely to be more specific than non-specific downstream effects on ^{18}F-FDG (16-18).

Amino acid metabolism in lung cancer

Malignant cells demonstrate an increase in cellular proliferation along with an increase in amino acid transport (carrier mediated transport processes) and protein metabolism. These processes can be imaged through radiolabelled amino acids such as ^{11}C-methionine and ^{18}F-tyrosine, which are essential amino acids (19).

The cellular uptake of large neutral amino acids is mediated by Na+ independent L-type amino acid transporters (LAT). Currently, 4 isoforms of system L transporters have been identified: LAT1, LAT2, LAT3, and LAT4. LAT1 is widely expressed in lung cancer amongst other primary human tumours of various tissue origins (20). LAT1 is upregulated in malignant tumours, and its expression is associated with tumour proliferation.

Unlike ^{18}F-FDG, radiolabelled amino acids have almost no tracer uptake in normal brain and as oncological PET tracers, have been used predominantly in the assessment of brain tumours (21). ^{11}C methionine may reduce the number of false-positive findings in inflammatory lung disorders as it is more specific for malignancy than ^{18}F-FDG. Several papers, from countries with endemic infective and inflammatory lung disorders, have looked at the possible diagnostic contribution of ^{11}C-methioinine PET in differentiating benign and malignant lung nodules (22) with both Kubota et al. (23) and Hsieh et al. (24) reporting that ^{11}C-methionine is more specific and sensitive when compared to ^{18}F-FDG.

^{18}F labelled *O*-(2-^{18}F-fluoroethyl)-L-tyrosine (^{18}F-FET) has shown results similar to those obtained with ^{11}C methionine in imaging brain tumours(25) and also demonstrated superior of human solid gliomas compared with MRI as shown by use of stereotactic biopsy samples as a reference (26). A recent study by Pauleit et al. has showed that ^{18}F-FDG PET, ^{18}F-FET PET may allow a better distinction between tumours and inflammatory tissues in patients with squamous cell carcinomas (21)l-3-18F-α-methyl tyrosine (^{18}F-FAMT) has been developed as a PET radiopharmaceutical for tumour amino acid imaging. ^{18}F-FAMT is almost exclusively transported by the LAT1, making it more specific for malignant tissue (20). Clinical studies have demonstrated that ^{18}F-FAMT exhibits higher cancer specificity in peripheral organs than other amino acid PET tracers and ^{18}F-FDG. Kaira et al. showed that metabolic response on ^{18}F-FAMT PET was a significant independent prognostic factor and could be a potential parameter to predict the prognosis after first-line chemotherapy in patients with advanced lung cancer (20).

Hypoxia in lung cancer

Tumour response to treatment has been shown to be significantly influenced by tumour hypoxia and oxygen metabolism. Intra-tumoral hypoxia increases radio-resistance and chemo-resistance, requiring an increase of 2.5–3 times the radiotherapy dose to achieve the same biological effect (27). It is also associated with poor clinical outcomes in solid tumours, including lung cancer (28-31).

^{18}F-fluoromisonidazole (^{18}F-FMISO), initially used in nuclear cardiology to assess myocardial ischaemia, was the first PET radiopharmaceutical introduced into oncological imaging armamentarium to measure tumour oxygenation in several cancer types including lung cancer (Fig. 3), sarcomas, brain tumours and head and neck cancers (32, 33). ^{18}F-FMISO enters cells by passive diffusion and is thought to undergo metabolism similar to MISO, being reduced by nitroreductase enzymes to form reduction products. These then bind to intracellular macromolecules when the oxygen tension is less than 10 mmHg and is then trapped intracellularly (34, 35). ^{18}F-FMISO is lipophilic and is excreted via the hepatobiliary route with pronounced liver and gut uptake. It does not accumulate in necrotic tissues, as the trapping process requires viable cells with functional nitroreductase enzymes (36). Limitations include slow tracer accumulation leading to low tumour-to-background contrast requiring delayed scans to allow background activity to decrease (37). Parameters used to quantify tumour hypoxia include tumour-to-blood uptake ratio (TBR) at 2 hours after injection using a cut off of 1.2 or 1.4 (38) (although TBR continues to increase up to 6 hours) (39) and standardised uptake value (SUV) and hypoxic fraction (HF, the fraction of pixels within the imaged tumour volume) (37).

Several preclinical and clinical studies have shown moderate correlations between direct oxygen electrode measurements and uptake of ^{18}F-FMISO. Clinical studies have shown ^{18}F-FMISO selectivity in NSCLC but the mechanism for how radiotherapy affects intratumoural oxygenation status remains uncertain. So far, only very weak correlations have been demonstrated between ^{18}F-FMISO and ^{18}F-FDG uptake and so further evaluation of the relationship between hypoxia and glucose metabolism is required (40-44). The feasibility of multi-tracer PET/CT scans performed in a short period of time prior to and during radiotherapy permits more sophisticated individualisation of NSCLC treatment. Further studies using larger cohorts and relating findings to patient outcomes are required (45).

Development of further hypoxic tracers has been driven by the presence of a suboptimal signal-to-background ratio of ^{18}F-FMISO. These include 2- nitroimidazoles like ^{18}F-fluoroazomycin arabinoside (^{18}F-FAZA), which has a better TBR and is excreted via the renal route (46, 47). Studies have shown that uptake of ^{18}F-FAZA and ^{18}F-FDG differ in NSCLC, confirming that these tracers assess different intratumoural biological processes (37). Another hypoxia tracer is ^{18}F-labeled fluoroerythronitroimidazole (18F-FETNIM). Clinical studies have shown the feasibility of ^{18}F-FETNIM PET and its potential as a prognostic marker in NSCLC (37). ^{18}F-3-fluoro-2-(4-((2-nitro-1H-imidazol-1-yl) methyl)-1H-1,2,3-triazol-1-yl) propan-1-ol (18F-HX4) is an another 2-nitroimidazole analogue, which owing to its high-water solubility and fast clearance from the non-hypoxic tissues, gives a better TBR. In a recent study by Zeger et al. it showed considerable uptake in the majority of NSCLC patients in their study group (48).

Alongside nitromidazole radiopharmaceuticals, the other most frequently used PET radiopharmaceutical is ^{64}Cu-methylthiosemicarbazone (^{64}Cu-ATSM). It is a neutral lipophilic molecule with a high cell membrane permeability and diffuses readily from the blood to surrounding cells. Once within the cell, it undergoes reduction only in hypoxic cells and becomes trapped intracellularly, but washes out rapidly from normal cells without any change (49). Copper has several positron-emitting radioisotopes which can be used. ^{64}Cu, because of its long half-life of 12.7 hours, is most frequently used and is suitable for long-distance distribution. ^{60}Cu ($t_{1/2}$ 24 mins) and ^{62}Cu ($t_{1/2}$ 9.7 mins), with short half-lives, allow serial imaging within a short time period to assess acute changes in hypoxia, e.g. due to therapeutic intervention. Due to conflicting correlative evidence with invasive oxygen measurements, the question as to whether Cu-ATSM is a true hypoxic imaging agent remains unanswered. The timing of image acquisition is important, as the initial phase of tracer uptake can be influenced by perfusion, whereas at later time points uptake is probably more indicative of tumour hypoxia, but later still may reflect trafficking of released copper following metabolism of the tracer.

Clinical studies have shown that ^{64}Cu-ATSM PET is feasible in NSCLC and may play a role as a prognostic marker (37, 49-52).

Angiogenesis in lung cancer

Angiogenesis is the complex biological process by which new blood vessels are formed and which has a vital role in the process of primary tumour growth, proliferation and metastasis. Angiogenesis is a highly-controlled process that is dependent on the intricate balance of numerous molecular pathways that involve several mediators, such as hypoxia-inducible factor 1 (HIF-1), matrix metalloproteinases (MMPs), $\alpha_v\beta_3$ integrin, E-selectin and growth factors/growth factor receptors, like vascular endothelial growth factor (VEGF), platelet-derived growth factor (PDGF) and fibroblast growth factor-2 (FGF-2), (53). These pathways are important targets for cancer therapeutics and hence imaging(54). PET offers a number of methods to quantify the angiogenic process in tumours.

Tumour blood flow can be measured using ^{15}O-H_2O, steady-state method described by Frackowiak et al., and the ^{15}O-dynamic water method described by Lammertsma et al. (54).

In association with tumour angiogenesis, integrins (a family of cell adhesion molecules), including $\alpha_v\beta_3$, are upregulated on activated endothelial cells. To date, most clinical studies have focused on targeted integrin PET imaging (1) of which $\alpha_v\beta_3$ integrin is the most extensively investigated imaging target in the integrin family. Integrin $\alpha_v\beta_3$ binds to a variety of extracellular matrix (ECM) molecules via the arginine-glycine-aspartic acid (RGD) sequence on ligands. The first generation RGD peptide tracers were mainly excreted by the hepatobiliary system, hence were associated with high background hepatobiliary and intestinal activity. In addition, the aspartic acid residue of RGD was found to be susceptible to degradation. Cyclisation and glycosylation of these cyclic RGD peptides further improved their pharmacokinetics. Second generation peptides, such as RGD-K5, are predominantly excreted by the kidneys with increased uptake and retention in tumours improving their imaging characteristics (55-59).

RGD peptides can be labelled with ^{18}F, ^{68}Ga or ^{64}Cu for PET imaging. Pre-clinical studies have confirmed that ^{18}F-labelled RGD has good tumour specificity and is rapidly cleared via renal excretion (60, 61). Two of the most investigated monomeric RGD peptides are ^{18}F-Galacto-RGD and ^{18}F-Fluciclatide, (formerly known as AH111585).

^{18}F-Galacto-RGD PET uptake correlates with immunohistological staining of $\alpha_v\beta_3$ integrin. Beer et al. conducted a study comparing the SUVs of ^{18}F-Galacto-RGD PET with ^{18}F-FDG PET in NSCLC (n=10). Although no correlation was found, they suggested further evaluation of ^{18}F-galacto-RGD PET for planning and response evaluation of targeted molecular therapies with antiangiogenic or $\alpha_v\beta_3$-targeted drugs (62). Metz et al. performed a prospective study on 13 patients with primary or metastasised cancer (NSCLC, n = 9; others, n = 4), analysing the spatial relationship of $\alpha_v\beta_3$ expression, glucose metabolism and perfusion by PET and dynamic contrast-enhanced (DCE) MRI, focusing on tumour heterogeneity (63). This study found that regions with simultaneous high uptake of ^{18}F-Galacto-RGD and ^{18}F-FDG also showed higher functional MRI perfusion parameters (gadopentetate dimeglumine concentration time curve (IAUGC), regional blood volume (rBV) and regional blood flow (rBF)), compared to areas with low uptake of both radiotracers. Concerning perfusion and $\alpha_v\beta_3$ expression, their results showed a tendency toward higher values for all functional MRI parameters in areas with more intense ^{18}F-galacto-RGD uptake than ^{18}F-FDG. This was thought to be because glucose metabolism is upregulated in hypoxic cells (which may occur in poorly perfused tumours) (63).

^{18}F-Fluciclatide, binds to $\alpha_v\beta_3$ and $\alpha_v\beta_5$ integrins with high affinity and in a preclinical study was found to bind to Lewis lung carcinoma and Calu-6 NSCLC xenografts in mice, with favourable biodistribution

properties that allow the non-invasive assessment of tumour vascularity and response to treatments that affect the tumour vascular compartment (61).

Attempts at optimising the strategies in labelling peptides with ^{18}F led to the development of ^{18}F-fluoride–aluminium complexes to radiolabel peptides such as ^{18}F-AlF-NOTA-PRGD2 (^{18}F-alfatide) (64). ^{18}F-alfatide has shown promising imaging properties and pharmacokinetics that are comparable, or superior, to those of other monomeric and dimeric RGD peptides. In a pilot study, by Wan et al., including nine patients with lung cancer, ^{18}F-Alfatide allowed identification of all tumours with SUVs of 2.9 ± 0.1 indicating a lower variance in tumour uptake than found by most other studies using RGD-derivatives in patients (64). Another pilot study by Zhou et al. also suggested that ^{18}F-Alfatide PET/CT potentially had a valuable role in the diagnosis of metastatic lymph nodes for NSCLC patients (65).

Due to increasing availability, ^{64}Cu and ^{68}Ga have generated interest for labelling peptides, resulting in the introduction of a variety of radiopharmaceuticals labelled with these radionuclides. DOTA-conjugated RGD peptide (DOTA-RGDyK) has been labelled with ^{64}Cu (66). ^{68}Ga NOTA-RGD is the first ^{68}Ga-labeled integrin-targeting compound for which initial clinical data is available. A study by Zheng et al. suggested that the diagnostic value of ^{68}Ga-NOTA-PRGD2 for lung cancer diagnosis was comparable to ^{18}F-FDG with a significant advantage over ^{18}F-FDG in identifying metastatic lymph nodes with greater specificity (67).

There is direct activation of the angiogenesis pathway by angiogenic factors, which include vascular endothelial growth factor (VEGF/VEGFR). The critical role of VEGF in cancer progression has been highlighted by the use of the humanised anti-VEGF monoclonal antibody bevacizumab (Avastin) for cancer treatment which has demonstrated a two-month survival benefit compared to doublet chemotherapy alone in advanced NSCLC (68). However, no clinical studies using targeted PET or imaging of VEGF/VEGFR in lung cancer are available in the literature (1), although there is preclinical data showing the feasibility of VEGFR PET imaging, especially with radiolabelled specific antibodies.

The extracellular matrix (ECM) also plays a role in neovascularisation. Matrix metalloproteinases (MMP) are proteolytic enzymes that degrade the basement membrane and ECM, facilitating endothelial cell migration during angiogenesis (54). MMP inhibitors have also been investigated as a therapeutic strategy in lung cancer. Marimastat, a synthetic MMP inhibitor, has been investigated in randomised controlled trials in stage III NSCLC and small cell lung cancer (SCLC), but failed to show any survival benefit with maintenance therapy. PET imaging using MMP-inhibitors has been investigated in the pre-clinical setting, although results from in vivo animal studies have not been promising (69-71).

Another pro-angiogenic factor in the ECM is fibronectin, which is involved in wound healing, cell migration and malignant transformation. The extra-domain B (ED-B) isoform of fibronectin localises to new vessels in a variety of proliferating solid animal tumour models including SCLC, as well as ocular angiogenesis and tumour healing. There are, however, no pre-clinical ED-B imaging studies in lung tumour models (37).

Epidermal growth factor (EGFR) – Tyrosine kinase inhibitor (TKI) treatment strategies for NSCLC depend on the mutation status of EGFR (72). A recent study by Sun et al. demonstrated N-(3-chloro-4-fluorophenyl)-7-(2-(2-(2-(2-18F-fluoroethoxy) ethoxy) ethoxy) ethoxy)-6-methoxyquinazolin-4-amine (^{18}F-MPG) PET/CT is a powerful method for precise quantification of EGFR-activating mutation status in NSCLC patients, and it is a promising strategy for noninvasively identifying patients sensitive to EGFR-TKIs and for monitoring the efficacy of EGFR-TKI therapy (72).

Radiopharmaceuticals in Pulmonary Neuroendocrine Tumours

^{18}F-Dihydroxyphenylalanine (^{18}F-DOPA) has been used as a PET radiopharmaceutical for in vivo imaging of the dopaminergic system in neurological disorders (73) since the 1980s. Later this radiopharmaceutical found use in the detection of malignancies such as brain tumours (74) and for detecting primary and metastatic disease of neuroendocrine differentiation (carcinoids, gastroenteropancreatic tumours, glomus tumours, medullary thyroid cancer, small cell lung cancer, and phaeochromocytoma) (75, 76). Neuroendocrine tumours (NETs) have been found to over produce an enzyme dihydrophenylalanine decarboxylase which metabolises ^{18}F-DOPA (77). ^{18}F-DOPA PET may be used to characterise pulmonary nodules with neuroendocrine components and to evaluate treatment response, but the literature is sparse (78, 79).

NETs express somatostatin receptors (SSTRs) on their cell membrane and thus far, six SSTR subtypes have been described namely SSTR1, SSTR2A, SSTR2B, SSTR3, SSTR4 and SSTR5. The SSTR2 and SSTR5 subtypes, in particular, are predominantly over-expressed on the cell membranes of NETs (on average in 80–90% of cases) whilst normal tissues express SSTR3 and SSTR5 subtypes (80). ^{68}Ga has a favourable half-life of 68 minutes and is obtained from a generator which can last a number of months. ^{68}Ga-DOTA somatostatin analogues were developed for clinical purposes (81) with several ^{68}Ga-DOTA-peptides available for clinical use including; ^{68}Ga-DOTA-Phe(1)-Tyr(3)-Octreotide (TOC), ^{68}Ga-DOTA-NaI(3)-Octreotide (NOC), and ^{68}Ga-DOTA-Tyr(3)-Octreotate (TATE). The main difference among these three tracers (DOTA-TOC, DOTA-NOC, and DOTA-TATE) is their variable affinity to SSTR subtypes. All of them show a similar affinity for SSTR2 and 5, whereas ^{68}Ga-DOTA-NOC demonstrates a high affinity for SSTR3 (82, 83). ^{68}Ga-DOTA-peptides are reported to be excellent candidates for imaging and staging patients with NETs, including the localisation of primary tumours in patients with known NET metastases (carcinoma of unknown primary origin) (84, 85) with sensitivities and specificities of 97-100% and 96-100%, respectively (86, 87) with a large series reporting a superior diagnostic accuracy to CT. 68-DOTA peptides can be used to characterise pulmonary nodules with a suspected neuroendocrine aetiology (Fig. 4, 5) (77). Kayani et al. reviewed cases of pulmonary NET who underwent both ^{68}Ga-DOTATATE and ^{18}F-FDG PET/CT and showed that typical bronchial carcinoids showed higher and more selective uptake of ^{68}Ga-DOTATATE compared to ^{18}F-FDG, whilst atypical carcinoids and higher grades demonstrated less ^{68}Ga-DOTATATE uptake but were ^{18}F-FDG-avid (88).

In a recent prospective study by Walker et al. they investigated indeterminate pulmonary nodules (IPN) using both ^{68}Ga-DOTATATE and ^{18}F-FDG PET/CT. The found that both tracers had equivalent accuracy in the diagnosis of malignant nodules. ^{68}Ga-DOTATATE was more specific (94% compared to 81%) and less sensitive (73% compared to 93%) than ^{18}F-FDG. Immunohistochemistry staining for SSTR2A receptor expression correlated with tumour stroma but not tumour cells (89).

Radiopharmaceuticals in imaging programmed cell death-ligand (PD-L1)

PD-L1 immune checkpoint inhibitors have changed the treatment options in advanced NSCLC which often demonstrate PD-L1 expression (90). There is a correlation between PD-L1 expression detected by immunohistochemistry and the response and progression free survival following PD-L1 monoclonal antibody treatment, such as nivolumab (91). Non-invasive quantification of PD-L1 expression in order to guide treatment is a current area of interest with some levels of success. A recent 13 patient trial by Niemeijer et al. (92) reported that in vivo imaging of the PD1/PD-L1 axis in NSCLC using ^{18}F-BMS-986192, an ^{18}Fluor-labeled anti-PD-L1 Adectin and ^{89}Zirconium-labeled nivolumab (^{89}Zr-nivolumab), was feasible and safe in humans and could be used in PD-L1 expression quantification. There are other pre-clinical trials looking at different PD-L receptor expression (93).

Conclusions

^{18}F-FDG PET/CT, which assesses cellular glycolytic metabolism, has a very high sensitivity and has an established role in the management of lung malignancy. There are several other radiopharmaceuticals available to investigate different cellular and molecular processes in malignancy such as proliferation, amino acid metabolism, hypoxia and angiogenesis, which in turn improves characterisation of tumours and treatment response assessment. However, the use of these radiopharmaceuticals remains largely restricted to the research arena and are yet to be adopted into routine clinical practice. Radiopharmaceuticals used to evaluate NETs have an established role in clinical practice but their success is reliant upon sufficient SSTR expression on tumour cells. In vivo PD-L1 expression quantification in NSCLC using different radiotracers might be the key to unlock newer immune checkpoint inhibitor treatments.

Acknowledgements

The authors acknowledge financial support from the King's College London / University College London Comprehensive Cancer Imaging Centres funded by Cancer Research UK and Engineering and Physical Sciences Research Council in association with the Medical Research Council and the Department of Health (C1519/A16463) and the Wellcome Trust EPSRC Centre for Medical Engineering at King's College London (WT203148/Z/16/Z).

Figure Legends

Figure 1a:

^{18}F-FLT PET/CT: CT (lung windows) and fused PET/CT axial images shows FLT uptake in a left upper lobe lung nodule. Physiological uptake is present in the bone marrow.

Figure 1b:

^{18}F-FDG PET/CT: CT (lung windows) and fused PET/CT axial image show the left upper lobe nodule is FDG avid, with greater uptake than the FLT scan.

Figure 2:

Post radiotherapy recurrent disease.

^{18}F-FDG PET/CT: CT (soft tissue windows), PET and fused PET/CT axial images (left) and ^{18}F-FLT PET/CT PET and fused PET/CT axial images (right)

The ^{18}F-FLT study shows more focal uptake in the left anteromedial segment, with non-avid background consolidation.

^{18}F-FDG study shows heterogenous inflammatory FDG in left lower lobar consolidation with more intense uptake in the left anteromedial segment corresponding to recurrent tumour uptake also seen on the FLT scan.

Figure 3:

^{18}F-FMISO PET/CT images 4 h p.i. on an SUV scale 0 – 3 for two different patients (courtesy and with permission McGowan DR, Macpherson RE, Hackett SL, Liu D, Gleeson FV, McKenna WG, et al. (18) F-fluoromisonidazole uptake in advanced stage non-small cell lung cancer: A voxel-by-voxel PET kinetics study. Med Phys. 2017 Sep;44(9):4665-76).

Figure 4a:

^{18}F-FDG PET/CT: CT (lung windows), PET and fused PET/CT axial image. A patient with a known neuroendocrine pancreatic tumour with a lung nodule. No significant FDG activity is present in keeping with low glycolytic activity in a well-differentiated tumour.

Figure 4b:

^{68}Ga-Dotatate PET/CT: CT (lung windows), PET and fused PET/CT axial image. High uptake in the nodule is in keeping with a well-differentiated tumour with somatostatin receptor expression.

Figure 5:

^{68}Ga-Dotatate PET/CT: axial image fused PET/CT, PET, CT (lung windows) and half body MIP showing an intensely avid well differentiated neuroendocrine tumour in the right upper lobe.

References

1. Szyszko TA, Yip C, Szlosarek P, Goh V, Cook GJ. The role of new PET tracers for lung cancer. Lung Cancer. 2016 Apr;94:7-14.

2. RefGrab-It Install Page [Internet]. [cited 12/16/2018]. Available from: http://www.refworks.com/refgrabit/rw2linkpage.aspx?subscriber=2721&user=25682&_=1544978109356.

3. Barthel H, Perumal M, Latigo J, He Q, Brady F, Luthra SK, et al. The uptake of 3'-deoxy-3'-[18F]fluorothymidine into L5178Y tumours in vivo is dependent on thymidine kinase 1 protein levels. Eur J Nucl Med Mol Imaging. 2005 Mar;32(3):257-63.

4. Shields AF, Grierson JR, Dohmen BM, Machulla HJ, Stayanoff JC, Lawhorn-Crews JM, et al. Imaging proliferation in vivo with [F-18]FLT and positron emission tomography. Nat Med. 1998 Nov;4(11):1334-6.

5. Rasey JS, Grierson JR, Wiens LW, Kolb PD, Schwartz JL. Validation of FLT uptake as a measure of thymidine kinase-1 activity in A549 carcinoma cells. J Nucl Med. 2002 Sep;43(9):1210-7.

6. Shields AF. Positron emission tomography measurement of tumor metabolism and growth: its expanding role in oncology. Mol Imaging Biol. 2006 May-Jun;8(3):141-50.

7. Buck AK, Schirrmeister H, Hetzel M, Von Der Heide M, Halter G, Glatting G, et al. 3-deoxy-3-[(18)F]fluorothymidine-positron emission tomography for noninvasive assessment of proliferation in pulmonary nodules. Cancer Res. 2002 Jun 15;62(12):3331-4.

8. Yue J, Chen L, Cabrera AR, Sun X, Zhao S, Zheng F, et al. Measuring tumor cell proliferation with 18F-FLT PET during radiotherapy of esophageal squamous cell carcinoma: a pilot clinical study. J Nucl Med. 2010 Apr;51(4):528-34.

9. Buck AK, Hetzel M, Schirrmeister H, Halter G, Moller P, Kratochwil C, et al. Clinical relevance of imaging proliferative activity in lung nodules. Eur J Nucl Med Mol Imaging. 2005 May;32(5):525-33.

10. Buck AK, Halter G, Schirrmeister H, Kotzerke J, Wurziger I, Glatting G, et al. Imaging proliferation in lung tumors with PET: 18F-FLT versus 18F-FDG. J Nucl Med. 2003 Sep;44(9):1426-31.

11. Yang W, Zhang Y, Fu Z, Yu J, Sun X, Mu D, et al. Imaging of proliferation with 18F-FLT PET/CT versus 18F-FDG PET/CT in non-small-cell lung cancer. Eur J Nucl Med Mol Imaging. 2010 Jul;37(7):1291-9.

12. Tian J, Yang X, Yu L, Chen P, Xin J, Ma L, et al. A multicenter clinical trial on the diagnostic value of dual-tracer PET/CT in pulmonary lesions using 3'-deoxy-3'-18F-fluorothymidine and 18F-FDG. J Nucl Med. 2008 Feb;49(2):186-94.

13. Sohn HJ, Yang YJ, Ryu JS, Oh SJ, Im KC, Moon DH, et al. 18F]Fluorothymidine positron emission tomography before and 7 days after gefitinib treatment predicts response in patients with advanced adenocarcinoma of the lung. Clin Cancer Res. 2008 Nov 15;14(22):7423-9.

14. Trigonis I, Koh PK, Taylor B, Tamal M, Ryder D, Earl M, et al. Early reduction in tumour [18F]fluorothymidine (FLT) uptake in patients with non-small cell lung cancer (NSCLC) treated with radiotherapy alone. Eur J Nucl Med Mol Imaging. 2014 Apr;41(4):682-93.

15. Allen MD, Luong P, Hudson C, Leyton J, Delage B, Ghazaly E, et al. Prognostic and therapeutic impact of argininosuccinate synthetase 1 control in bladder cancer as monitored longitudinally by PET imaging. Cancer Res. 2014 Feb 1;74(3):896-907.

16. Szlosarek PW, Luong P, Phillips MM, Baccarini M, Stephen E, Szyszko T, et al. Metabolic response to pegylated arginine deiminase in mesothelioma with promoter methylation of argininosuccinate synthetase. J Clin Oncol. 2013 Mar 1;31(7):e111-3.

17. Beddowes E, Spicer J, Chan PY, Khadeir R, Corbacho JG, Repana D, et al. Phase 1 Dose-Escalation Study of Pegylated Arginine Deiminase, Cisplatin, and Pemetrexed in Patients With Argininosuccinate Synthetase 1-Deficient Thoracic Cancers. J Clin Oncol. 2017 Jun 1;35(16):1778-85.

18. Szlosarek PW, Steele JP, Nolan L, Gilligan D, Taylor P, Spicer J, et al. Arginine Deprivation With Pegylated Arginine Deiminase in Patients With Argininosuccinate Synthetase 1-Deficient Malignant Pleural Mesothelioma: A Randomized Clinical Trial. JAMA Oncol. 2017 Jan 1;3(1):58-66.

19. Nariai T, Tanaka Y, Wakimoto H, Aoyagi M, Tamaki M, Ishiwata K, et al. Usefulness of L-[methyl-11C] methionine-positron emission tomography as a biological monitoring tool in the treatment of glioma. J Neurosurg. 2005 Sep;103(3):498-507.

20. Wiriyasermkul P, Nagamori S, Tominaga H, Oriuchi N, Kaira K, Nakao H, et al. Transport of 3-fluoro-L-alpha-methyl-tyrosine by tumor-upregulated L-type amino acid transporter 1: a cause of the tumor uptake in PET. J Nucl Med. 2012 Aug;53(8):1253-61.

21. Pauleit D, Stoffels G, Schaden W, Hamacher K, Bauer D, Tellmann L, et al. PET with O-(2-18F-Fluoroethyl)-L-Tyrosine in peripheral tumors: first clinical results. J Nucl Med. 2005 Mar;46(3):411-6.

22. Swensen SJ, Jett JR, Hartman TE, Midthun DE, Mandrekar SJ, Hillman SL, et al. CT screening for lung cancer: five-year prospective experience. Radiology. 2005 Apr;235(1):259-65.

23. Kubota K, Yamada K, Fukada H, Endo S, Ito M, Abe Y, et al. Tumor detection with carbon-11-labelled amino acids. Eur J Nucl Med. 1984;9(3):136-40.

24. Hsieh HJ, Lin SH, Lin KH, Lee CY, Chang CP, Wang SJ. The feasibility of 11C-methionine-PET in diagnosis of solitary lung nodules/masses when compared with 18F-FDG-PET. Ann Nucl Med. 2008 Jul;22(6):533-8.

25. Weber WA, Wester HJ, Grosu AL, Herz M, Dzewas B, Feldmann HJ, et al. O-(2-[18F]fluoroethyl)-L-tyrosine and L-[methyl-11C]methionine uptake in brain tumours: initial results of a comparative study. Eur J Nucl Med. 2000 May;27(5):542-9.

26. Messing-Junger AM, Floeth FW, Pauleit D, Reifenberger G, Willing R, Gartner J, et al. Multimodal target point assessment for stereotactic biopsy in children with diffuse bithalamic astrocytomas. Childs Nerv Syst. 2002 Aug;18(8):445-9.

27. GRAY LH, CONGER AD, EBERT M, HORNSEY S, SCOTT OC. The concentration of oxygen dissolved in tissues at the time of irradiation as a factor in radiotherapy. Br J Radiol. 1953 Dec;26(312):638-48.

28. Vaupel P, Mayer A. Hypoxia in cancer: significance and impact on clinical outcome. Cancer Metastasis Rev. 2007 Jun;26(2):225-39.

29. Hockel M, Vorndran B, Schlenger K, Baussmann E, Knapstein PG. Tumor oxygenation: a new predictive parameter in locally advanced cancer of the uterine cervix. Gynecol Oncol. 1993 Nov;51(2):141-9.

30. Nordsmark M, Overgaard M, Overgaard J. Pretreatment oxygenation predicts radiation response in advanced squamous cell carcinoma of the head and neck. Radiother Oncol. 1996 Oct;41(1):31-9.

31. Wilhelm R, Kovacs G, Heinrichsohn D, Galalae R, Kimmig B. Survival of exclusively irradiated patients with NSCLC. Significance of pretherapeutic hemoglobin level. Strahlenther Onkol. 1998 Mar;174(3):128-32.

32. Hicks RJ, Rischin D, Fisher R, Binns D, Scott AM, Peters LJ. Utility of FMISO PET in advanced head and neck cancer treated with chemoradiation incorporating a hypoxia-targeting chemotherapy agent. Eur J Nucl Med Mol Imaging. 2005 Dec;32(12):1384-91.

33. Rajendran JG, Wilson DC, Conrad EU, Peterson LM, Bruckner JD, Rasey JS, et al. (18)F]FMISO and [(18)F]FDG PET imaging in soft tissue sarcomas: correlation of hypoxia, metabolism and VEGF expression. Eur J Nucl Med Mol Imaging. 2003 May;30(5):695-704.

34. Rasey JS, Grunbaum Z, Magee S, Nelson NJ, Olive PL, Durand RE, et al. Characterization of radiolabeled fluoromisonidazole as a probe for hypoxic cells. Radiat Res. 1987 Aug;111(2):292-304.

35. Prekeges JL, Rasey JS, Grunbaum Z, Krohn KH. Reduction of fluoromisonidazole, a new imaging agent for hypoxia. Biochem Pharmacol. 1991 Nov 27;42(12):2387-95.

36. Lee ST, Scott AM. Hypoxia positron emission tomography imaging with 18f-fluoromisonidazole. Semin Nucl Med. 2007 Nov;37(6):451-61.

37. Yip C, Blower PJ, Goh V, Landau DB, Cook GJ. Molecular imaging of hypoxia in non-small-cell lung cancer. Eur J Nucl Med Mol Imaging. 2015 May;42(6):956-76.

38. Michalski MH, Chen X. Molecular imaging in cancer treatment. Eur J Nucl Med Mol Imaging. 2011 Feb;38(2):358-77.

39. Peeters SG, Zegers CM, Lieuwes NG, van Elmpt W, Eriksson J, van Dongen GA, et al. A comparative study of the hypoxia PET tracers [(1)(8)F]HX4, [(1)(8)F]FAZA, and [(1)(8)F]FMISO in a preclinical tumor model. Int J Radiat Oncol Biol Phys. 2015 Feb 1;91(2):351-9.

40. Koh WJ, Bergman KS, Rasey JS, Peterson LM, Evans ML, Graham MM, et al. Evaluation of oxygenation status during fractionated radiotherapy in human nonsmall cell lung cancers using [F-18]fluoromisonidazole positron emission tomography. Int J Radiat Oncol Biol Phys. 1995 Sep 30;33(2):391-8.

41. Koh WJ, Rasey JS, Evans ML, Grierson JR, Lewellen TK, Graham MM, et al. Imaging of hypoxia in human tumors with [F-18]fluoromisonidazole. Int J Radiat Oncol Biol Phys. 1992;22(1):199-212.

42. Rasey JS, Koh WJ, Evans ML, Peterson LM, Lewellen TK, Graham MM, et al. Quantifying regional hypoxia in human tumors with positron emission tomography of [18F]fluoromisonidazole: a pretherapy study of 37 patients. Int J Radiat Oncol Biol Phys. 1996 Sep 1;36(2):417-28.

43. Gagel B, Reinartz P, Demirel C, Kaiser HJ, Zimny M, Piroth M, et al. 18F] fluoromisonidazole and [18F] fluorodeoxyglucose positron emission tomography in response evaluation after chemo-/radiotherapy of non-small-cell lung cancer: a feasibility study. BMC Cancer. 2006 Mar 4;6:51,2407-6-51.

44. Eschmann SM, Paulsen F, Reimold M, Dittmann H, Welz S, Reischl G, et al. Prognostic impact of hypoxia imaging with 18F-misonidazole PET in non-small cell lung cancer and head and neck cancer before radiotherapy. J Nucl Med. 2005 Feb;46(2):253-60.

45. Vera P, Bohn P, Edet-Sanson A, Salles A, Hapdey S, Gardin I, et al. Simultaneous positron emission tomography (PET) assessment of metabolism with (1)(8)F-fluoro-2-deoxy-d-glucose (FDG), proliferation with (1)(8)F-fluoro-thymidine (FLT), and hypoxia with (1)(8)fluoro-misonidazole (F-miso) before and during radiotherapy in patients with non-small-cell lung cancer (NSCLC): a pilot study. Radiother Oncol. 2011 Jan;98(1):109-16.

46. Sorger D, Patt M, Kumar P, Wiebe LI, Barthel H, Seese A, et al. 18F]Fluoroazomycinarabinofuranoside (18FAZA) and [18F]Fluoromisonidazole (18FMISO): a comparative study of their selective uptake in hypoxic cells and PET imaging in experimental rat tumors. Nucl Med Biol. 2003 Apr;30(3):317-26.

47. Piert M, Machulla HJ, Picchio M, Reischl G, Ziegler S, Kumar P, et al. Hypoxia-specific tumor imaging with 18F-fluoroazomycin arabinoside. J Nucl Med. 2005 Jan;46(1):106-13.

48. Zegers CM, van Elmpt W, Wierts R, Reymen B, Sharifi H, Ollers MC, et al. Hypoxia imaging with [(1)(8)F]HX4 PET in NSCLC patients: defining optimal imaging parameters. Radiother Oncol. 2013 Oct;109(1):58-64.

49. Knight JC, Wuest M, Saad FA, Wang M, Chapman DW, Jans HS, et al. Synthesis, characterisation and evaluation of a novel copper-64 complex with selective uptake in EMT-6 cells under hypoxic conditions. Dalton Trans. 2013 Sep 7;42(33):12005-14.

50. Dehdashti F, Mintun MA, Lewis JS, Bradley J, Govindan R, Laforest R, et al. In vivo assessment of tumor hypoxia in lung cancer with 60Cu-ATSM. Eur J Nucl Med Mol Imaging. 2003 Jun;30(6):844-50.

51. Lohith TG, Kudo T, Demura Y, Umeda Y, Kiyono Y, Fujibayashi Y, et al. Pathophysiologic correlation between 62Cu-ATSM and 18F-FDG in lung cancer. J Nucl Med. 2009 Dec;50(12):1948-53.

52. Dehdashti F, Grigsby PW, Mintun MA, Lewis JS, Siegel BA, Welch MJ. Assessing tumor hypoxia in cervical cancer by positron emission tomography with 60Cu-ATSM: relationship to therapeutic response-a preliminary report. Int J Radiat Oncol Biol Phys. 2003 Apr 1;55(5):1233-8.

53. Niccoli Asabella A, Di Palo A, Altini C, Ferrari C, Rubini G. Multimodality Imaging in Tumor Angiogenesis: Present Status and Perspectives. Int J Mol Sci. 2017 Aug 28;18(9):10.3390/ijms18091864.

54. Niu G, Chen X. PET Imaging of Angiogenesis. PET Clin. 2009 Jan 1;4(1):17-38.

55. Su ZF, Liu G, Gupta S, Zhu Z, Rusckowski M, Hnatowich DJ. In vitro and in vivo evaluation of a Technetium-99m-labeled cyclic RGD peptide as a specific marker of alpha(V)beta(3) integrin for tumor imaging. Bioconjug Chem. 2002 May-Jun;13(3):561-70.

56. Bogdanowich-Knipp SJ, Jois DS, Siahaan TJ. The effect of conformation on the solution stability of linear vs. cyclic RGD peptides. J Pept Res. 1999 May;53(5):523-9.

57. Dijkgraaf I, Boerman OC. Molecular imaging of angiogenesis with SPECT. Eur J Nucl Med Mol Imaging. 2010 Aug;37 Suppl 1:S104-13.

58. Beer AJ, Kessler H, Wester HJ, Schwaiger M. PET Imaging of Integrin alphaVbeta3 Expression. Theranostics. 2011 Jan 17;1:48-57.

59. Haubner R, Wester HJ, Burkhart F, Senekowitsch-Schmidtke R, Weber W, Goodman SL, et al. Glycosylated RGD-containing peptides: tracer for tumor targeting and angiogenesis imaging with improved biokinetics. J Nucl Med. 2001 Feb;42(2):326-36.

60. Haubner R, Wester HJ, Weber WA, Mang C, Ziegler SI, Goodman SL, et al. Noninvasive imaging of alpha(v)beta3 integrin expression using 18F-labeled RGD-containing glycopeptide and positron emission tomography. Cancer Res. 2001 Mar 1;61(5):1781-5.

61. Morrison MS, Ricketts SA, Barnett J, Cuthbertson A, Tessier J, Wedge SR. Use of a novel Arg-Gly-Asp radioligand, 18F-AH111585, to determine changes in tumor vascularity after antitumor therapy. J Nucl Med. 2009 Jan;50(1):116-22.

62. Kossodo S, Pickarski M, Lin SA, Gleason A, Gaspar R, Buono C, et al. Dual in vivo quantification of integrin-targeted and protease-activated agents in cancer using fluorescence molecular tomography (FMT). Mol Imaging Biol. 2010 Oct;12(5):488-99.

63. Metz S, Ganter C, Lorenzen S, van Marwick S, Herrmann K, Lordick F, et al. Phenotyping of tumor biology in patients by multimodality multiparametric imaging: relationship of microcirculation, alphavbeta3 expression, and glucose metabolism. J Nucl Med. 2010 Nov;51(11):1691-8.

64. Wan W, Guo N, Pan D, Yu C, Weng Y, Luo S, et al. First experience of 18F-alfatide in lung cancer patients using a new lyophilized kit for rapid radiofluorination. J Nucl Med. 2013 May;54(5):691-8.

65. Zhou Y, Gao S, Huang Y, Zheng J, Dong Y, Zhang B, et al. A Pilot Study of (18)F-Alfatide PET/CT Imaging for Detecting Lymph Node Metastases in Patients with Non-Small Cell Lung Cancer. Sci Rep. 2017 Jun 6;7(1):2877,017-03296-6.

66. Chen X, Park R, Tohme M, Shahinian AH, Bading JR, Conti PS. MicroPET and autoradiographic imaging of breast cancer alpha v-integrin expression using 18F- and 64Cu-labeled RGD peptide. Bioconjug Chem. 2004 Jan-Feb;15(1):41-9.

67. Zheng K, Liang N, Zhang J, Lang L, Zhang W, Li S, et al. 68Ga-NOTA-PRGD2 PET/CT for Integrin Imaging in Patients with Lung Cancer. J Nucl Med. 2015 Dec;56(12):1823-7.

68. Sandler A, Gray R, Perry MC, Brahmer J, Schiller JH, Dowlati A, et al. Paclitaxel-carboplatin alone or with bevacizumab for non-small-cell lung cancer. N Engl J Med. 2006 Dec 14;355(24):2542-50.

69. Furumoto S, Takashima K, Kubota K, Ido T, Iwata R, Fukuda H. Tumor detection using 18F-labeled matrix metalloproteinase-2 inhibitor. Nucl Med Biol. 2003 Feb;30(2):119-25.

70. Zheng QH, Fei X, Liu X, Wang JQ, Stone KL, Martinez TD, et al. Comparative studies of potential cancer biomarkers carbon-11 labeled MMP inhibitors (S)-2-(4'-[11C]methoxybiphenyl-4-sulfonylamino)-3-methylbutyric acid and N-hydroxy-(R)-2-[[(4'-[11C]methoxyphenyl)sulfonyl]benzylamino]-3-methylbutanamide. Nucl Med Biol. 2004 Jan;31(1):77-85.

71. Oltenfreiter R, Staelens L, Labied S, Kersemans V, Frankenne F, Noel A, et al. Tryptophane-based biphenylsulfonamide matrix metalloproteinase inhibitors as tumor imaging agents. Cancer Biother Radiopharm. 2005 Dec;20(6):639-47.

72. Sun X, Xiao Z, Chen G, Han Z, Liu Y, Zhang C, et al. A PET imaging approach for determining EGFR mutation status for improved lung cancer patient management. Sci Transl Med. 2018 Mar 7;10(431):10.1126/scitranslmed.aan8840.

73. Garnett ES, Firnau G, Nahmias C. Dopamine visualized in the basal ganglia of living man. Nature. 1983 Sep 8-14;305(5930):137-8.

74. Heiss WD, Wienhard K, Wagner R, Lanfermann H, Thiel A, Herholz K, et al. F-Dopa as an amino acid tracer to detect brain tumors. J Nucl Med. 1996 Jul;37(7):1180-2.

75. Becherer A, Szabo M, Karanikas G, Wunderbaldinger P, Angelberger P, Raderer M, et al. Imaging of advanced neuroendocrine tumors with (18)F-FDOPA PET. J Nucl Med. 2004 Jul;45(7):1161-7.

76. Nanni C, Fanti S, Rubello D. 18F-DOPA PET and PET/CT. J Nucl Med. 2007 Oct;48(10):1577-9.

77. Maffione AM, Grassetto G, Rampin L, Chondrogiannis S, Marzola MC, Ambrosini V, et al. Molecular imaging of pulmonary nodules. AJR Am J Roentgenol. 2014 Mar;202(3):W217-23.

78. Ambrosini V, Tomassetti P, Castellucci P, Campana D, Montini G, Rubello D, et al. Comparison between 68Ga-DOTA-NOC and 18F-DOPA PET for the detection of gastro-entero-pancreatic and lung neuro-endocrine tumours. Eur J Nucl Med Mol Imaging. 2008 Aug;35(8):1431-8.

79. Caroli P, Nanni C, Rubello D, Alavi A, Fanti S. Non-FDG PET in the practice of oncology. Indian J Cancer. 2010 Apr-Jun;47(2):120-5.

80. Bombardieri E, Maccauro M, De Deckere E, Savelli G, Chiti A. Nuclear medicine imaging of neuroendocrine tumours. Ann Oncol. 2001;12 Suppl 2:S51-61.

81. Hofmann M, Maecke H, Borner R, Weckesser E, Schoffski P, Oei L, et al. Biokinetics and imaging with the somatostatin receptor PET radioligand (68)Ga-DOTATOC: preliminary data. Eur J Nucl Med. 2001 Dec;28(12):1751-7.

82. Prasad V, Baum RP. Biodistribution of the Ga-68 labeled somatostatin analogue DOTA-NOC in patients with neuroendocrine tumors: characterization of uptake in normal organs and tumor lesions. Q J Nucl Med Mol Imaging. 2010 Feb;54(1):61-7.

83. Maecke HR, Hofmann M, Haberkorn U. (68)Ga-labeled peptides in tumor imaging. J Nucl Med. 2005 Jan;46 Suppl 1:172S-8S.

84. Baum RP, Prasad V, Hommann M, Horsch D. Receptor PET/CT imaging of neuroendocrine tumors. Recent Results Cancer Res. 2008;170:225-42.

85. Prasad V, Ambrosini V, Hommann M, Hoersch D, Fanti S, Baum RP. Detection of unknown primary neuroendocrine tumours (CUP-NET) using (68)Ga-DOTA-NOC receptor PET/CT. Eur J Nucl Med Mol Imaging. 2010 Jan;37(1):67-77.

86. Gabriel M, Decristoforo C, Kendler D, Dobrozemsky G, Heute D, Uprimny C, et al. 68Ga-DOTA-Tyr3-octreotide PET in neuroendocrine tumors: comparison with somatostatin receptor scintigraphy and CT. J Nucl Med. 2007 Apr;48(4):508-18.

87. Ambrosini V, Nanni C, Zompatori M, Campana D, Tomassetti P, Castellucci P, et al. (68)Ga-DOTA-NOC PET/CT in comparison with CT for the detection of bone metastasis in patients with neuroendocrine tumours. Eur J Nucl Med Mol Imaging. 2010 Apr;37(4):722-7.

88. Kayani I, Conry BG, Groves AM, Win T, Dickson J, Caplin M, et al. A comparison of 68Ga-DOTATATE and 18F-FDG PET/CT in pulmonary neuroendocrine tumors. J Nucl Med. 2009 Dec;50(12):1927-32.

89. Walker R, Deppen S, Smith G, Shi C, Lehman J, Clanton J, et al. 68Ga-DOTATATE PET/CT imaging of indeterminate pulmonary nodules and lung cancer. PLoS One. 2017 Feb 9;12(2):e0171301.

90. Zhang M, Wang D, Sun Q, Pu H, Wang Y, Zhao S, et al. Prognostic significance of PD-L1 expression and (18)F-FDG PET/CT in surgical pulmonary squamous cell carcinoma. Oncotarget. 2017 May 29;8(31):51630-40.

91. Niemeijer AN, Smit EF, Dongen GaMSv, Windhorst AD, Huisman MC, Hendrikse NH, et al. Whole body PD-1 and PD-L1 PET with 89Zr-nivolumab and 18F- BMS-986192 in pts with NSCLC. JCO. 2017 05/20; 2018/12;35(15):e20047-.

92. Niemeijer A, Leung D, Huisman M,C., Bahce I, Hoekstra O, van Dongen G,A.M.S., et al. Whole body PD-1 and PD-L1 positron emission tomography in patients with non-small-cell lung cancer. ; 2018.

93. Truillet C, Oh HLJ, Yeo SP, Lee CY, Huynh LT, Wei J, et al. Imaging PD-L1 Expression with ImmunoPET. Bioconjug Chem. 2018 Jan 17;29(1):96-103.

The role of new PET tracers for lung cancer

Figure 1a:

^{18}F-FLT PET/CT: CT (lung windows) and fused PET/CT axial images

Shows a FLT avid left upper lobe lung nodule. Physiological uptake in the bone marrow.

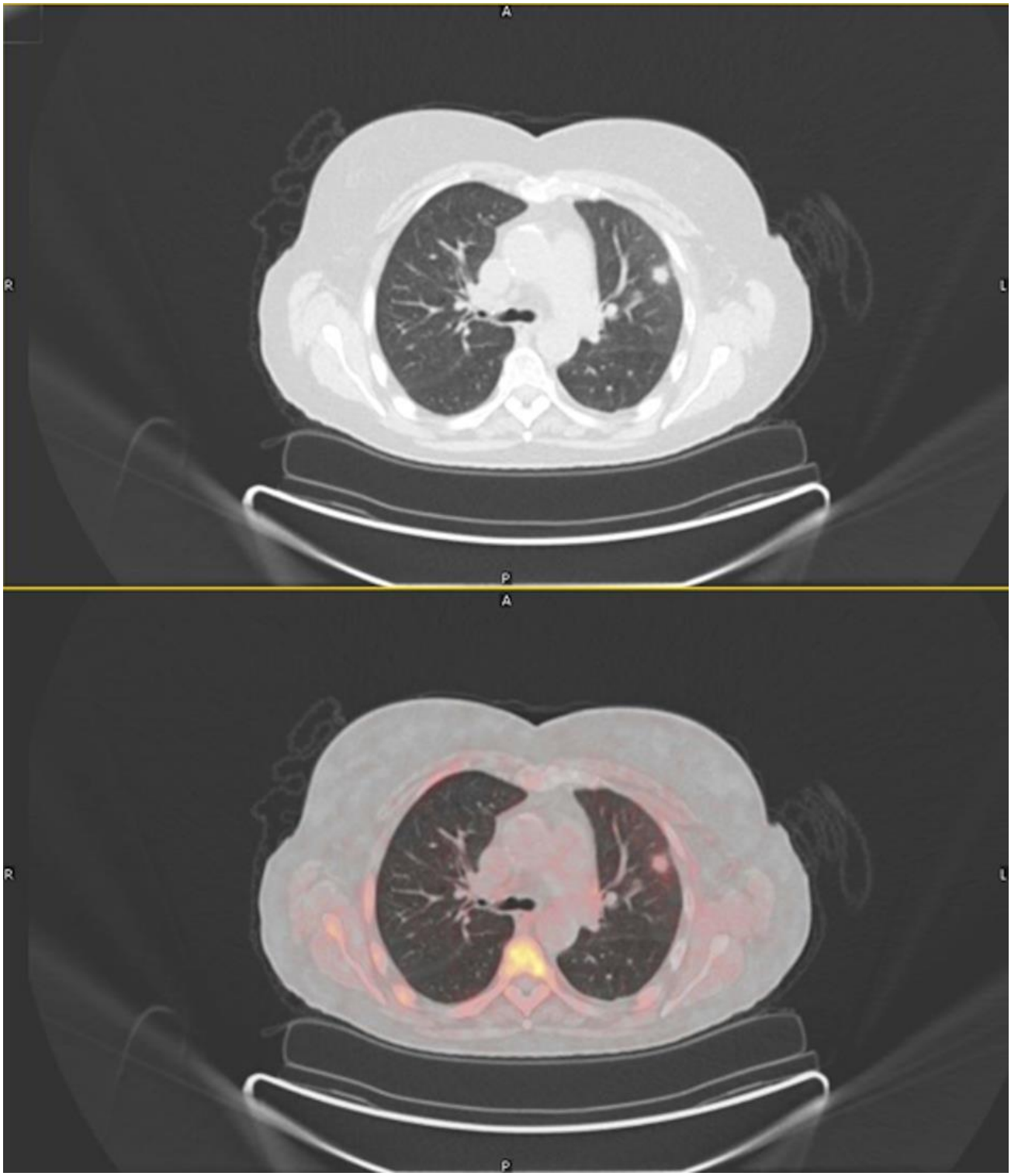

Figure 1b:

^{18}F-FDG PET/CT: CT (lung windows) and fused PET/CT axial image

Show the left upper lobe nodule is FDG avid.

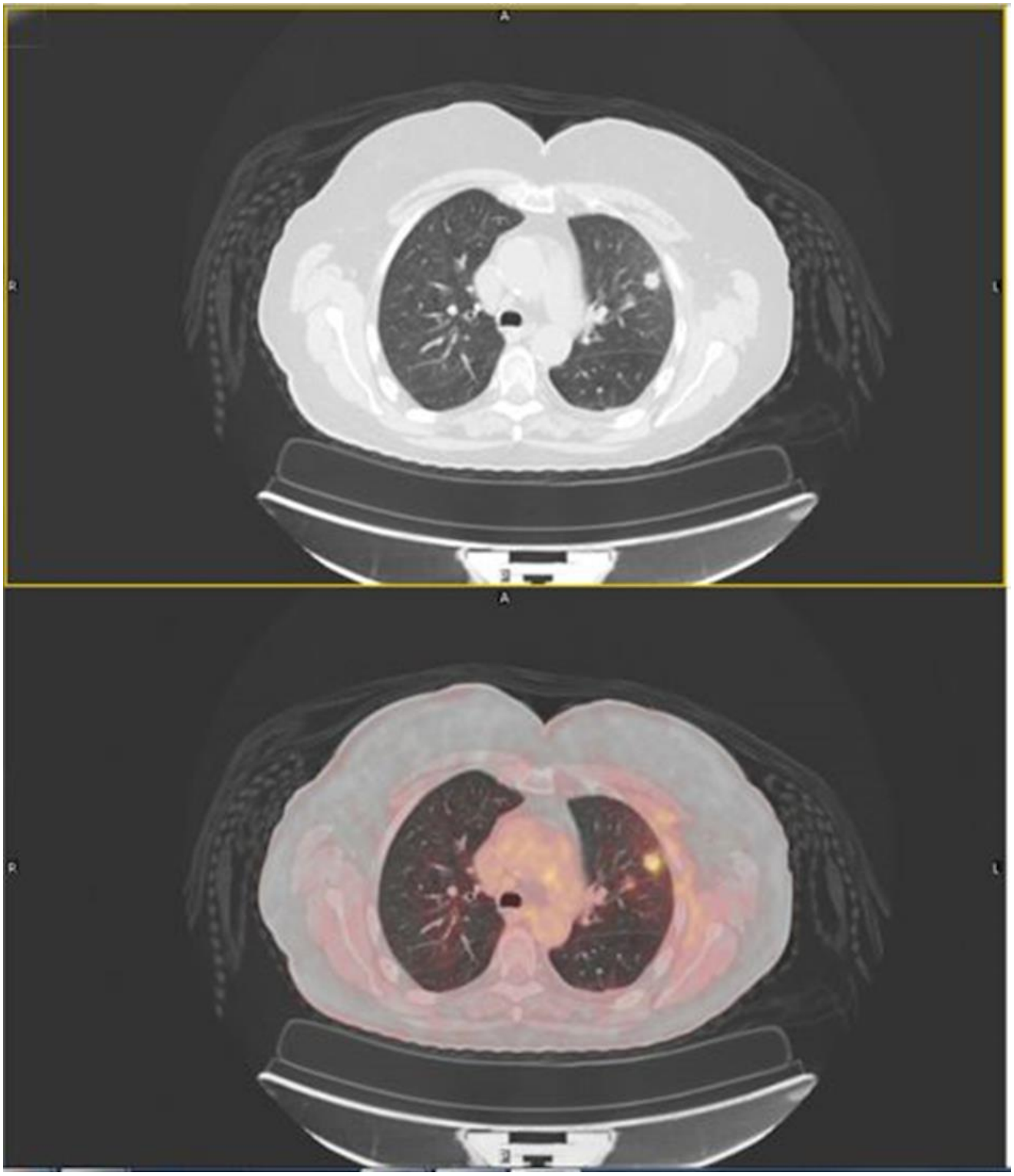

Figure 2:

Post radiotherapy recurrent disease.

^{18}F-FDG PET/CT: CT(soft tissue windows), PET and fused PET/CT axial images along with ^{18}F-FLT PET/CT PET and fused PET/CT axial images

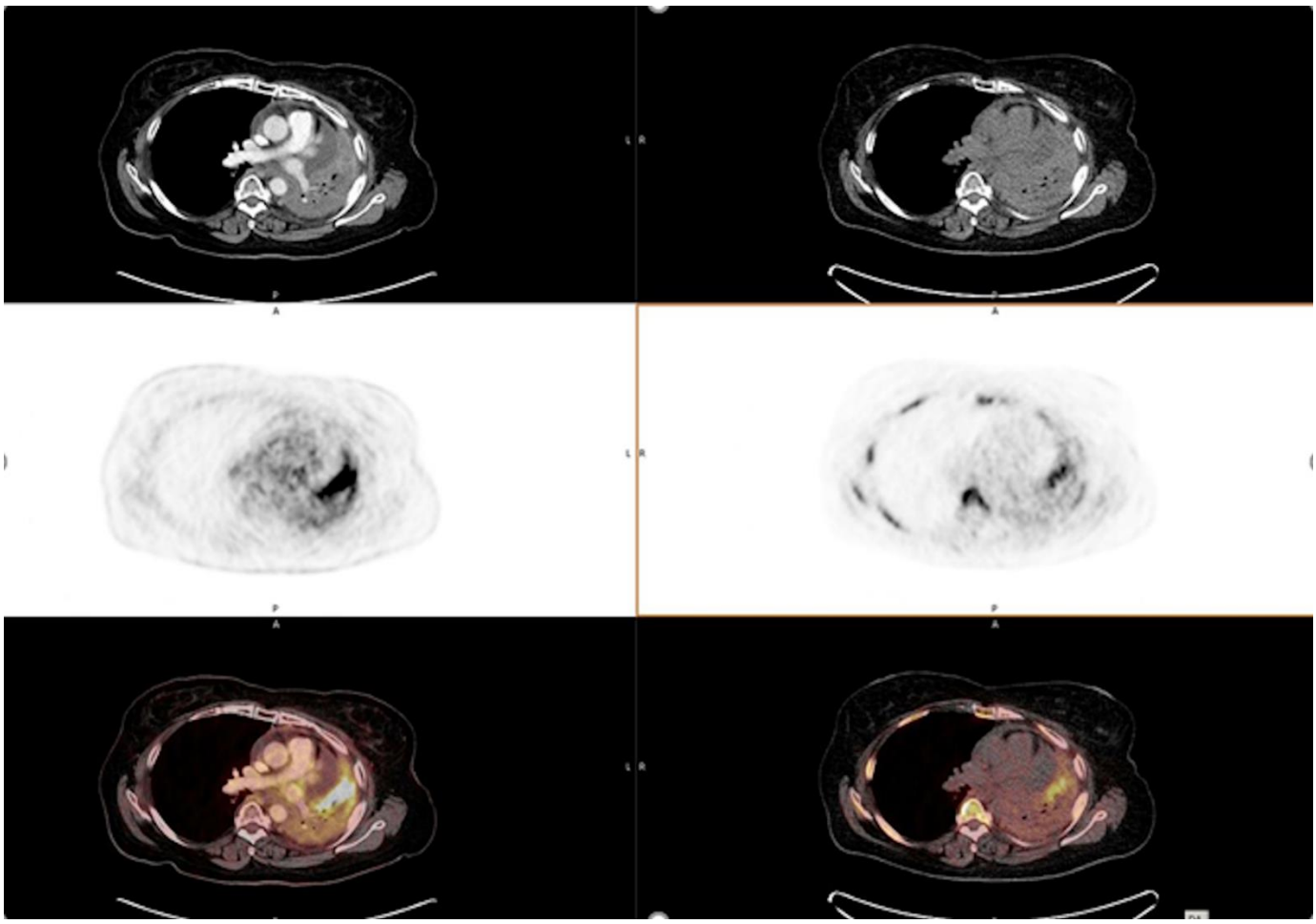

^{18}F-FDG study shows heterogenous FDG in left lower lobar consolidation with more intense uptake in the left anteromedial segment.

^{18}F-FLT study shows more focal FDG avidity in the left anteromedial segment, with non-avid background consolidation.

Figure 3:

^{18}F-FMISO PET/CT images 4 h p.i. (pre-Buparlisib) on an SUV scale 0 – 3 for two different patients(1)

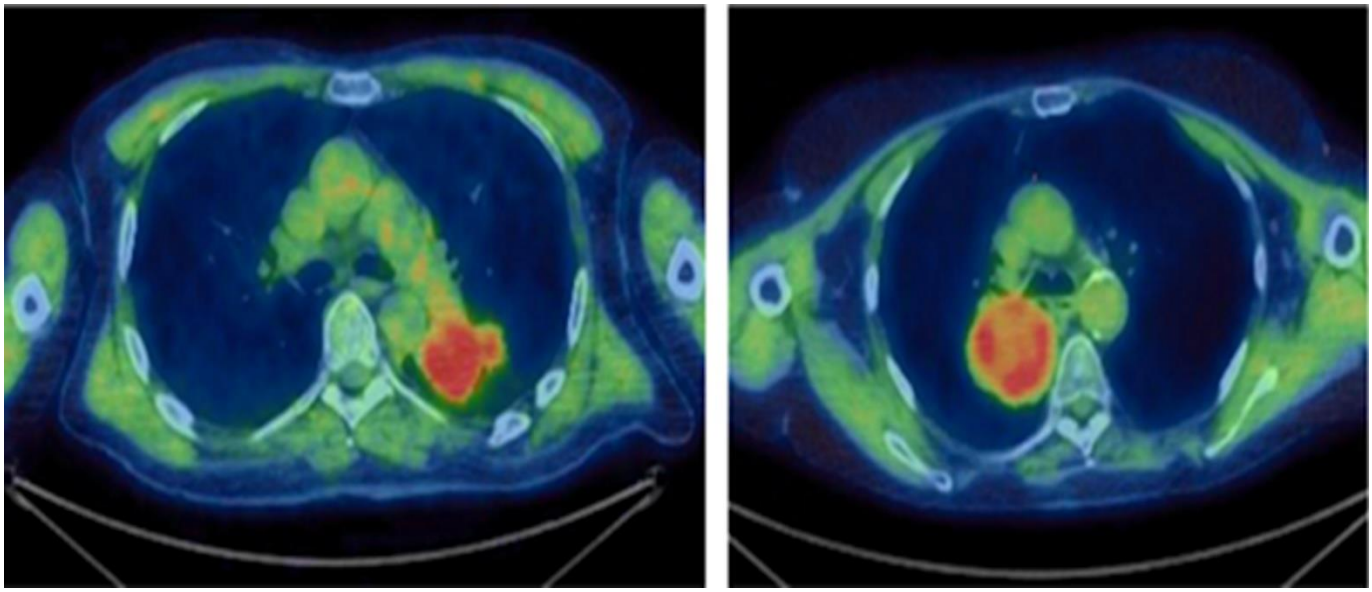

1. McGowan DR, Macpherson RE, Hackett SL, Liu D, Gleeson FV, McKenna WG, et al. (18) F-fluoromisonidazole uptake in advanced stage non-small cell lung cancer: A voxel-by-voxel PET kinetics study. Med Phys. 2017 Sep;44(9):4665-76.

Figure 4a:

^{18}F-FDG PET/CT: CT (lung windows), PET and fused PET/CT axial image. In a patient with known neuroendocrine pancreatic tumour with a lung nodule.

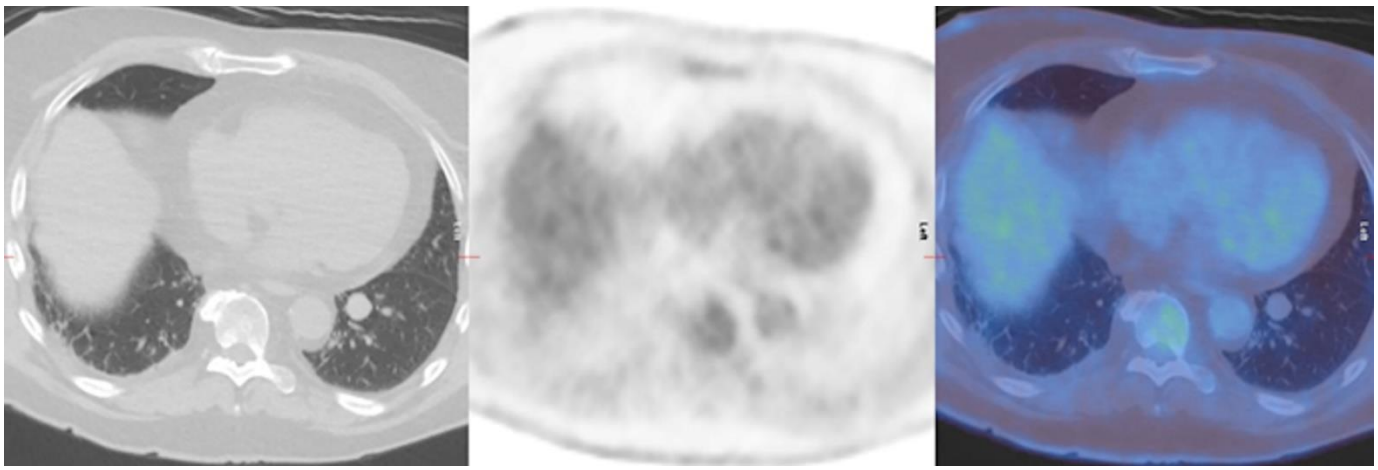

Figure 4b:

^{68}Ga-Dotatate PET/CT: CT (lung windows), PET and fused PET/CT axial image. In patient with known neuroendocrine pancreatic tumour with a lung nodule.

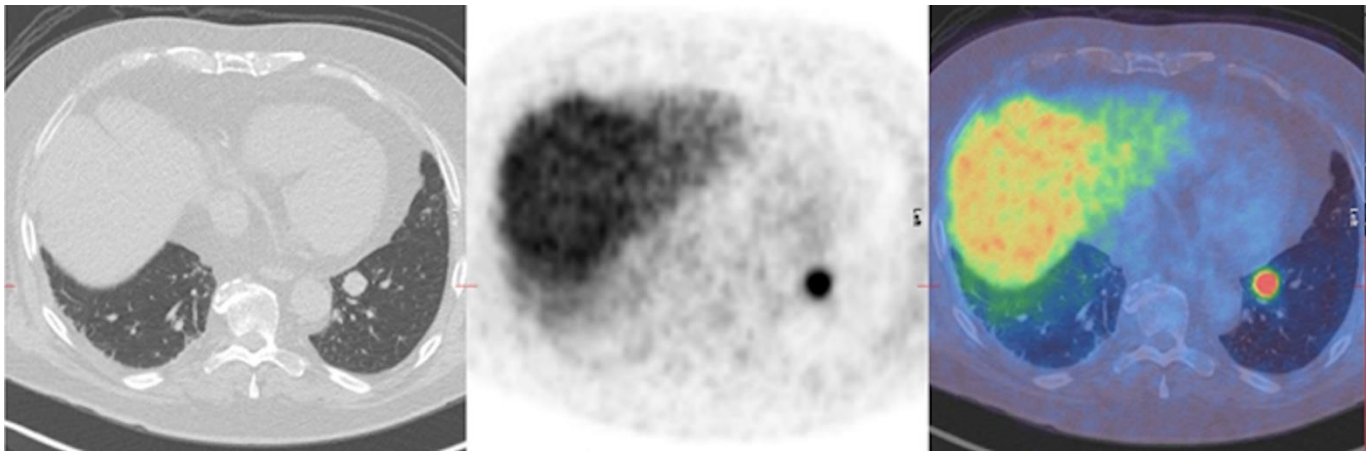

Figure 5:

^{68}Ga-Dotatate PET/CT: axial image fused PET/CT, PET, CT (lung windows) and half body MIP showing an intensely avid neuroendocrine tumour in the right upper lobe.